Can A Foreign Particle Cause Surface Instability?

X. Y. Liu, B. E. P. G. van den Berg, A. R. A. Zauner, and P. Bennema

Department of Physics, the National University of Singapore, 10 Kent Ridge Crescent, Singapore 119260

Received: May 17, 2000; In Final Form: September 21, 2000

The occurrence of foreign bodies on growing surfaces of crystals will serve as precursors for heterogeneous two-dimensional (2D) nucleation so that at relatively low supersaturations, it will promote rapid growth at the regions where the foreign particles are in contact with the crystal surface. This leads to so-called particle-induced surface instability. At high supersaturations, due to the limitation of effective transport, heterogeneous 2D nucleation will become kinetically unfavorable. Foreign particles have no effect on crystal growth. A heterogeneous 2D nucleation model is put forward to analyze this special type of surface instability. To check the model, we examined a naphthalene crystal-melt system experimentally. A novel phenomenon of a needlelike pattern of surface instability caused by solid-particle-induced growth was observed. This particle-induced surface instability occurs in a completely different regime of G/R from the dendritic-like surface instability. The theoretical predictions are confronted with the measured kinetic relations of the both normal and induced growth. The results turn out to be in excellent agreement with the predictions.

I. Introduction

The surface stability of growing crystals is of significant importance for materials science, industrial processing, and biomineralization.[1−3] This is because surface stability leads to the formation of various patterns of crystalline materials. These patterns, which are most likely to capture liquid between the branches, determine the liquid rheological and mechanical properties of the system. A decent understanding of the physics controlling of surface instability and pattern formation promises new routes of controlled synthesis of complex crystalline structures for applications across a broad spectrum of materials-based technologies.

When a liquid is supersaturated and begins to crystallize, the crystals grow and penetrate into the metastable liquid phase. The resulting crystallites often appear as needlelike dendrites,[1,2] similar in appearance to the arms of a snowflake.[3,4] Dendrites are a common morphology for diffusion-controlled crystal growth in the presence of anisotropy.[5−9] For the growth of crystals, some quantity that is generated at the interface between the crystal and melt during freezing—for example, the latent head of crystallization—must diffuse away from that interface. In the case where a very low or negative temperature gradient occurs in the liquid side of the interface like fins on a thermal radiator, the sharp tip of the dendrites may promote the diffusion of the head away from itself, allowing the crystal to grow rapidly in the direction in which the tip is pointing. When the ratio between the temperature gradient in the liquid phase G and the growth velocity of the crystal surface R is lower than a certain value, i.e

$$G/R < C \tag{1}$$

surface instability will occur.[1−4] (Here C is a constant for a given crystallization system). According to eq 1, the surface becomes less stable when G is more negative.

In general, the instability of growing crystal faces is due to a certain type of perturbation at the growing front, which triggers a local growth more rapid than the growth of the rest of the crystal surface. This rapid growth leads to a certain pattern, which is associated with the internal structure of crystals and the external conditions. As mentioned previously, the occurrence of surface instability is driven by the mass or heat diffusion.[1−4] However, whether foreign particles cause surface instability if they can promote the growth of the crystal surface they touch is a challenging question has never been addressed before.

In this paper, we will examine surface instability due to the occurrence of foreign particles. The requirement for such an understanding is due to the wide existence of foreign particles, ranging from solid dust particles and aggregates, gas or liquid bubbles, macro or polymer molecules, and secondary nuclei occurring during the growth of host crystals even to impurity molecules. This means that the influence of foreign particles on growth kinetics and, consequently, on surface instability is inevitable under normal conditions. The knowledge in this aspect will not only allow us to control effectively the surface instability, it will also permit the identification of new routes in controlling the quality and macroscopic properties of crystals and, furthermore, in promoting the growth of crystals and the pattern formation.

For the growth of crystals bounded by flat faces, due to the existence of a two-dimensional (2D) nucleation barrier ΔG_c (cf. section II), the growth of crystals occurs in a flat mode or layer-by-layer fashion at relatively low supersaturations σ (the supersaturation σ can be related to the thermodynamic driving force $\Delta\mu/kT$ as $\ln(1 + \sigma) = \Delta\mu/kT$, where $\Delta\mu$ is the difference in chemical potential between solute and solid units, k is the Boltzmann constant, and T is temperature).[10−12] This implies that the growth in the crystal surface is caused by the sweeping of advancing steps over the crystal surface layer by layer. In this case, a step where many kinks exist will serve as a sink where growth units are incorporated into the crystal structure. How step sources are generated turns out to be the rate-limiting step for the smooth growth.[10,11] Virtually any external disturbance capable of breaking down the 2D nucleation barrier will promote the growth of smooth crystal faces.

The growth of crystals bounded by facets usually occurs in either a spiral fashion (so-called screw dislocation mechanism), whereby one or more screw dislocations on the crystal surface

10.1021/jp001811s CCC: $19.00
Published on Web 11/18/2000

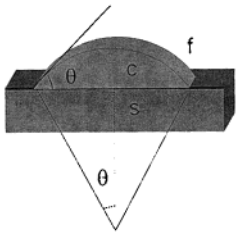

Figure 1. Schematic illustration of the heterogeneous 2D nucleation. Embryo "c" on nucleating particle "s" in mother phase "f".

give rise to spiral steps, or a birth-and-spread (so-called two-dimensional) fashion. The latter implies that the growth of the surfaces can be visualized as an alternative process of the spread of an existing layer on the surface and the creation of a new layer via a 2D nucleation process on the existing layer.[13−15] In the case of narrow flat crystal faces, such as the faceted {110} side faces of naphthalene crystals (cf. Figure 5), since dislocation lines at the surface can easily be terminated at the large top and the bottom faces, the {110} faces most likely become dislocation-free faces in the later stage of growth. Therefore, the growth can be controlled by 2D nucleation mechanisms.

Within the framework of the 2D nucleation mechanisms,[1,15] foreign particles touching the growing crystal surface are likely to serve as "substrates" for two-dimensional nucleation (called hereafter heterogeneous 2D nucleation). Consequently, the local growth rate of the surface may be enhanced. If these particles remain at the surface during the process of crystal growth, the promoting effect will consequently cause a certain type of surface instability, which will be referred hereafter as particle-induced surface instability.

In this paper, we will put forward a new model to describe the effect of foreign particles on the surface morphological stability of growing crystal faces. Experimentally, both morphological observations and quantitative measurements on the particle-induced surface growth at the {110} faces of naphthalene crystals from the melt and of n-$C_{32}H_{66}$ crystals grown from n-hexane solutions will be presented.

II. Theory

The model to be presented is a so-called heterogeneous 2D nucleation model. This model is based on the following assumptions: (1) the crystal surface is essentially flat and perfect, and (2) foreign particles in touch with the crystals surface have a much larger radius than the critical size of nuclei. This means that foreign particles can be considered to have straight edges (very small curvature in comparison with 2D nuclei; see Figure 1).

A. Effect of Foreign Particles on Free Energy Barrier of 2D Nucleation. The process of 2D nucleation on a crystal surface can be visualized as follows: transient visiting molecules adsorb, form short-lived unions, break-up, desorb, etc., in the boundary region of foreign particles. An instantaneous census would show some distributions of subcritical nuclei (or embryos) with 1, 2, 3, ... molecules per embryo. (Embryos are the metastable clusters of structural units with a broad distribution in size. The formation of stable crystal nuclei result from the fluctuation and "growth" of these embryos.)[14,15] In any embryo with g molecules, the free energy changes when the g molecules adsorb and form the g-mer with the size of r. Nucleation begins with the formation of an embryo of size r_c with g_c molecules. Similar to 3D nucleation, 2D nucleation will occur by surpassing the 2D nucleation barrier.

As shown in Figure 1, we denote the mother phase by subscript f, the embryo by c, and the foreign particle by s. If we denote volume by V and surface area of the edge by S, then the free energy of formation of an embryo with radius r on a nucleating particle with radius R^s is given by

$$\Delta G = -\frac{S_{sc}}{\Omega}\Delta\mu + (L_{cf}\gamma_{cf}^{step} + L_{cs}\gamma_{cf}^{step} - L_{cs}\gamma_{sf}^{step}) \qquad (2)$$

with

$$S_{sc} = \frac{1}{2}r^2(2\theta - 2\cos\theta\sin\theta) = r^2[\arccos m - (1-m^2)^{1/2}m] \qquad (3)$$

$$L_{cf} = 2r\arccos m \qquad (4)$$

$$L_{cs} = 2r\sin\theta = 2r(1-m^2)^{1/2} \qquad (5)$$

and

$$m = \cos\theta = (\gamma_{sc}^{step} - \gamma_{sf}^{step})/\gamma_{cf}^{step} \qquad (6)$$

(cf. Figure 1.) Here, γ_{ij}^{step} is the step free energy of the edge between phases i and j, and Ω is the volume per structural unit.

Equation 2 implies that the change in Gibbs free energy ΔG due to 2D nucleation is controlled by two counter effects. On one hand, the transformation of structural units from the liquid to 2D embryos at the growing crystal surface will lower ΔG by $S_{sc}/\Omega\Delta\mu$. On the other hand, the growth of 2D embryos will lengthen their circumference, leading to an increase in the total step energy and, consequently, ΔG. The second effect will be reduced when the 2D nucleation occurs at the edge of foreign particles. This is due to the interaction between nucleating layers and foreign particles that compensates for the increase in the total step free energy. Taking the effect of foreign particles into account, we describe the second effect by $(L_{cf}\gamma_{cf}^{step} + L_{cs}\gamma_{cf}^{step} - L_{cs}\gamma_{sf}^{step})$ in eq 2.

The combination of the first and the second effect gives rise to the following situation: in the case where the radius r of 2D embryos is smaller than a critical radius r_c, the expansion of 2D embryos leads to a rise in ΔG, while at $r > r_c$, the growth of the embryos lowers ΔG. ΔG at $r = r_c$ is defined as the 2D nucleation barrier ΔG_c, which in a sense is similar to the 3D nucleation barrier.[14] 2D nucleation actually is a process for 2D embryos to surpass the 2D nucleation barrier. The occurrence of foreign particles on the growth surface may suppress this barrier and promote the kinetics within a certain range of supersaturations. In the following part, we will establish the correlations of ΔG_c and r_c with other parameters.

Substituting eqs 3−6 into eq 2 yields

$$\Delta G = \Delta G_{homo} f(m) \qquad (7)$$

$$\Delta G_{homo} = -\frac{r^2 h}{\Omega}\pi\Delta\mu + 2r\pi\gamma_{cf}^{step} \qquad (8)$$

and

$$f(m) = \left[\frac{\arccos m - m(1-m^2)^{1/2}}{\pi}\right] \qquad (9)$$

where ΔG_{homo} corresponds to the change in free energy in the homogeneous 2D nucleation process and h is the height of the steps at the crystal surface.

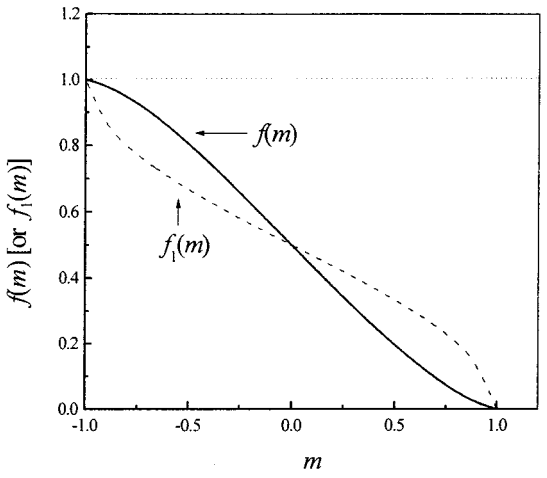

Figure 2. Factors $f(m)$ and $f_1(m)$ as functions of m. Both $f(m)$ and $f_1(m)$ decrease from 1 to 0 as m changes from -1 to 1.

To evaluate the critical free energy ΔG_c, we require that

$$(\partial \Delta G/\partial r)_c = 0 \tag{10}$$

It follows that the critical size of nuclei r_c is given by

$$r_c = \Omega\gamma_{cf}/\Delta\mu = \Omega\gamma_{cf}^{step}/kT \ln(1+\sigma) \tag{11}$$

Here, σ is the supersaturation, defined as $\sigma = (X_A - X_A^o)/X_A^o$; X_A and X_A^o represent the actual concentration and the equilibrium concentration of the solute, respectively.[10−12] Similarly, the free energy for the formation of critical embryo is obtained as

$$\Delta G^*_{induced} = \Delta G^*_{homo} f(m) \tag{12}$$

with

$$\Delta G^*_{homo} = \frac{\Omega(\gamma_{cf}^{step})^2 \pi h}{kT \ln(1+\sigma)} \tag{13}$$

Here, ΔG^*_{homo} corresponds to the free energy barrier of homogeneous 2D nucleation.[10]

It should be pointed out that not all foreign particles will promote 2D nucleation. The interfacial parameter m, which is determined by the step free energy γ_{ij}^{step} (cf. eq 6), will determine the effect of foreign particles on the nucleation kinetics. The is effect can be understood in terms of $f(m)$. In Figure 2, $f(m)$ is plotted as a function of m, which shows that $f(m)$ varies between 0 and 1. The case where $m = 1$ corresponds to the situation that the interaction and structural match between crystal steps and foreign particles is optimal. It follows that $f(m) = 0$ (see Figure 2), meaning that the 2D nucleation barrier is completely suppressed. At low supersaturation, the growth rate will be enhanced to the maximum at the given conditions. The case where $m = -1$ corresponds to the situation that foreign particles reveal negative (or repulsive) interactions with crystal steps. The result is then $f(m) = 1$ (see Figure 2), meaning that foreign particles have no effect on the growth of crystals.

B. Effect of Foreign Particles on Surface 2D Nucleation Kinetics and Growth Kinetics. The consideration of nucleation kinetics normally initiates from the distribution function of the concentrations of embryos of various sizes. We assume that a quasiequilibrium state exists on the surface between the monomers and g-mers.[16,17] Note that this state does not actually exist in any real process, but this approximation allows us to employ the tools of thermodynamics in our analysis.

We start by taking a basis of a unit length and defining the number of monomers, dimers, ..., and g-mers on this area to be $n_1, n_2, ..., n_g$. These equilibrium surface concentrations are time-invariant. Regarding the ensemble of monomers and g-mers on the surface and approximating the equilibrium with the following quasi chemical reaction equilibrium[17]

$$g \text{ monomer} \rightleftharpoons ... \rightleftharpoons g\text{-mer}$$

the expression

$$(n_g/Z) = (n_1/Z)^g \exp(-\Delta G_g/kT\} \tag{14}$$

can be easily obtained (for all g; $g = 2, 3, 4, ...$), with the effective total number of "molecules" per unit area defined by

$$Z = n_1 + \sum_{g=2} n_g \tag{15}$$

Here, ΔG_g denotes the free energy barrier to form a g-mer. Since usually $n_1 >>> \sum n_g$ ($g > 1$), $Z \sim n_1$; thus

$$n_g \cong n_1 \exp(-\Delta G_g/kT) \tag{16}$$

Equation 16 is usually the expression for the distribution of embryo sizes in supersaturated media.

We notice that embryos are not static entities in the microsense. Each particular one is growing larger or smaller as molecules are added to or leave the embryo, respectively. To obtain the rate of formation of critical-size embryos, we need to derive a general expression for the growth rate of a single embryo.[18]

Let α be the rate of molecule addition. That is

$$\alpha = \beta_{st}' \upsilon^{\neq} \tag{17}$$

where $\upsilon^{\neq}$ is the collision rate of monomers with an embryo and β_{st}' the sticking probability of the incoming structural units at the embryo, which is defined as

$$\beta_{st}' = \frac{a}{\lambda_o} \exp(-\Delta G_{step}^{\neq}/kT) \tag{18}$$

(a is the dimension of structural units in the direction parallel to the crystal surface, λ_o is the distance between two kinks at a step, and $\Delta G_{step}^{\neq}$ is the activation free energy for step integration). Also, let α' be the rate at which embryos lose molecules. Rates α and α' should be equal if the system is in equilibrium, since no embryo would then experience a net growth or disintegration. For an embryo of radius r, the value of α is determined by the surface concentration of monomers, n_1. Thus, at equilibrium

$$\alpha_g n_g - \alpha'_{g+1} n_{g+1} = 0 \tag{19}$$

On the other hand, if there is growth, then the equilibrium distribution is perturbed. Let f_g be this perturbed surface concentration of g-mers ($f_g \leq n_g$). Assuming a steady-state growth process, J^o, we find the formation rate of critical nuclei per unit area-time in the boundary region of an adsorbed foreign particle to be equal to the steady-state growth of embryos in the region of the surface. This can then be expressed as

$$J^o \equiv ... = \alpha_g f_g - \alpha'_{g+1} f_{g+1} = \text{constant} \tag{20}$$

The boundary conditions are as follows:

(1) $$f_{g_c} = 0 \tag{21}$$

(2) $$\lim_{g\to 1}(f_g/n_g) = 1 \tag{22}$$

The first is because whenever a $(g_c - 1)$-mer becomes a g_c-mer, it disappears from our population to begin a new stage—growth. But this event does not disturb the distribution of other embryos (mainly monomers). The second is because both n_g and f_g are large numbers when g is small. It follows that the perturbed concentration of monomers is almost equal to the equilibrium concentration.

Rearranging eq 20

$$J^o = \alpha_g n_g[(f_g/n_g) - (\alpha_g + 1/\alpha_g)(f_g + 1/n_g)] \tag{23}$$

and then using eq 19, we obtain

$$J^o = \alpha_g n_g[(f_g/n_g) - (f_g + 1/n_g + 1)] \tag{24}$$

Applying the steady-state condition (eq 20) and the boundary conditions (eqs 21 and 22) for embryos with all different sizes,[15] we obtain then the local nucleation rate J^o

$$J^o = [\int_1^{g_c}(\alpha_g n_g)^{-1}\,\mathrm{d}g]^{-1} \tag{25}$$

The evaluation of the integral in eq 25 is difficult, but it can be simplified by determining the dominant terms within the range from $g = 1$ to g_c. Certainly n_g decreases exponentially with g so that for large values of g the inverse n_g term is large. Therefore, the key is to find the variation of α_g with g.

According to eq 17, to find α_g, we need to derive an expression for $\upsilon^{\neq}$.

The number of monomers on the surface with speeds between υ and $\upsilon + \mathrm{d}\upsilon$ and directions between θ and $\theta + \mathrm{d}\theta$ is given by $f_\upsilon\,\mathrm{d}\upsilon f_\theta\,\mathrm{d}\theta$, where f_υ is the speed distribution function and f_θ the angular distribution function. If all angles are equally probable, $f_\theta = (1/2\pi)$.

For an embryo, the projected length visible to an external molecule is $\cos\theta\,\mathrm{d}L$ where $\mathrm{d}L$ is a differential element measured in on the periphery of the embryo.

The number of molecules colliding on the unit length of this embryo from all external surface adsorbed molecules, $\tilde{\upsilon}^{\neq}$, is then

$$\tilde{\upsilon}^{\neq} = 2n_1 K\int_0^{\pi/2}[(\cos\theta)/2\pi]\,\mathrm{d}\theta\int_0^{\infty}\upsilon f_\upsilon\,\mathrm{d}\upsilon \tag{26}$$

Note that K is introduced to describe the deviation due to the shape and surface anisotropy of foreign particles. $\int_0^{\infty}\upsilon f_\upsilon\,\mathrm{d}\upsilon$ is the average speed, $\bar{\upsilon}$. Integrating eq 26 and multiplying it by the arc length of the embryo, $2\pi r\psi/\pi$, yields

$$\upsilon^{\neq} = K\tilde{\upsilon}^{\neq}2\pi r\frac{\psi}{\pi} = 2rn_1\bar{\upsilon}K\frac{\psi}{\pi} \tag{27}$$

According to Figure 1, ψ can be given as

$$\psi = \arccos m \tag{28}$$

Obviously, $\upsilon^{\neq}$ (or α_g) increases as the square root of g. For large values of g, α_g is then only a weak function of g.

Returning to eq 25, we find that if the regions of high g contribute most and if, in these regions, α_g is not a strong function of g, then α_g may be removed from under the integral sign, and it can be approximated as a constant equal to its value when $r = r_c$, i.e.

$$\alpha_g \sim \alpha_{g_c} = 2\beta_{st}' r_c n_1 \bar{\upsilon} K\frac{\psi}{\pi} \tag{29}$$

As long as we have concluded that the important region for g in the integral of eq 25 is where $g \sim g_c$, we can simplify the evaluation by rewriting it as

$$(J^o)^{-1} = \alpha_{g_c}{}^{-1}\int^{g_c} n_g{}^{-1}\,\mathrm{d}g \tag{30}$$

and with eq 16

$$(J^o)^{-1} = (\alpha_{g_c} n_1)^{-1}\int^{g_c}\exp(\Delta G/kT)\,\mathrm{d}g \tag{31}$$

Expanding ΔG about g_c in a Taylor series and truncating after the second term, we find[15]

$$J^o = 2F_{g_c} n_{g_c}/(2\pi kT/Q)^{1/2} \tag{32}$$

$$Q = -(\partial^2\Delta G/\partial g^2)_{g=g_c} \tag{33}$$

where Q is positive so that the integral is an error function.

Henceforth the last remaining step is to evaluate Q. For the heterogeneous 2D nucleation the second derivative of ΔG is very complex. Note that the derivatives are evaluated at $g = g_c$ so are not a function of g. In most cases (x is small or is large), $f(m,x)$ turns out to be constant. We can approximate the value of $(\partial^2\Delta G/\partial g^2)_{g=g_c}$ by $f(m,x)(\partial^2\Delta G_{homo}/\partial g^2)_{g=g_c}$, therefore Q can be expressed as

$$Q \approx \gamma_{cf}^{step}(\pi h\Omega)^{1/2} f(m)/2g_c{}^{3/2} \tag{34}$$

or, with eq 8

$$Q \approx \gamma_{cf}^{step}\Omega^2 f(m)/2\pi h r_c{}^3 \tag{35}$$

By combing eqs 26, 27, 28, and 33, we obtain an expression for J. Thus, on the basis of eq 20

$$J^o = [\beta_{st}'(2r_c\bar{\upsilon}n_1)(2n_{g_c})/(2\pi kT)^{1/2}][\gamma_{cf}\Omega^2/2\pi h r_c{}^3]^{1/2} \times \left\{K\frac{\psi}{\pi}[f(m)]^{1/2}\right\} \tag{36}$$

Eliminating r_c with eq 8, we obtain

$$J^o = \left\{\frac{2\bar{\upsilon}n_1{}^2}{\pi}\left[\frac{\Omega\ln(1+\sigma)}{h}\right]^{1/2}\exp\left(\frac{-\Delta G_c}{kT}\right)\right\}\beta_{st}'\left\{K\frac{\psi}{\pi}[f(m)]^{1/2}\right\} \tag{37}$$

We notice that at the crystal surface[10,11]

$$\bar{\upsilon} \cong D_s = a\upsilon_{||}\exp(-\Delta G_{sdiff}^{\neq}/kT) \tag{38}$$

where $\Delta G_{deads}^{\neq}$ and $\upsilon_{||}$ are the potential barrier of deadsorption and the frequency of thermal vibration parallel for structural units,[3] respectively. If

$$f_1(m) = \left[\frac{\arccos m}{\pi}\right] \tag{39}$$

eq 36 is then rewritten as

$$J^{o} = \left\{\frac{2D_s n_1^{2}}{\pi}\left[\frac{\Omega \ln(1+\sigma)}{h}\right]^{1/2} \times \exp\left(-\frac{\Omega(\gamma_{cf}^{step})^2 \pi h}{(kT)^2 \ln(1+\sigma)} f(m)\right)\right\} K f_1(m)[f(m)]^{1/2} \quad (40)$$

In the equation, $f_1(m)$ is also a function of m, as shown in Figure 2.

Equation 40 includes also homogeneous 2D nucleation as a limited case. In the case of homogeneous 2D nucleation, $m \rightarrow -1$. It follows that $f_1(m) = f(m) = 1$, and $\{Kf_1(m)[f(m)]^{1/2}\}$. Equation 40 describes the rate of homogeneous 2D nucleation.

Having obtained the heterogeneous 2D nucleation rate, we can obtain the normal growth rate around foreign particles in contact with the crystal surface. Here, the best model to describe the growth kinetics of 2D nucleation is the birth and spread model.[16] According to this model, nucleation of the 2D crystal layer first occurs at a flat crystal surface and then follows simultaneously the growth of these nuclei and the formation of other critical nuclei. This model allows for both nucleation of critical-size embryos and subsequent growth at a finite rate. Therefore, we adapt the following three assumptions regarding the growth or spreading of the growing nuclei:[16] (a) there is no intergrowth between nuclei, (b) the lateral spreading velocity V_∞ is a constant, independent of the island size, and (c) nuclei can be born anywhere around foreign particles, which can occur on incomplete layers as well as on islands.

On the basis of this model, the growth rate can be given by[14,15]

$$R = h(J^{o})^{1/3}(V_\infty)^{2/3} \quad (41)$$

Now, finding the expression V_∞ is the key to obtaining R. Regarding the medium from which the crystal is grown, V_∞ will adapt different forms, according to the following two cases.

1. Growth of Crystals from Solution or Melt. In this case, the volume diffusion is the major way to transport the growth units from the bulk to the kinks on the surface. According to Chernov[1]

$$V_\infty = \pi\Omega\beta_{st} X_{hkl}^{o} \zeta\sigma \quad (42)$$

with $\zeta = [1 + (\pi\beta_{st}/D\lambda_s) \ln(\lambda_s/\pi a)]^{-1}$<id;reqid;43> where X_{hkl}^{o} is the equilibrium concentration of the solute at the crystal surface and is approximately equal to n_1, D is the volume diffusion constant, λ_s is the diffusion mean free path, and β_{st} is the kinetic coefficient for the step integration. The normal growth rate R is given, according to eqs 48, 41, and 42 as

$$R = C_1\sigma^{2/3}[\ln(1+\sigma)]^{1/6} \exp[-C_2 f(m)/T^2 \times \ln(1+\sigma)]\{Kf_1(m)[f(m)]^{1/2}\}^{1/3} \quad (44)$$

with

$$C_1 = (h\Omega)^{5/6}\beta_{st}[2D_s\pi/a\upsilon_{||}]^{1/3}[(n_1)^2\zeta]^{2/3} \quad (45)$$

and

$$C_2 = \frac{\Omega(\gamma_{cf}^{step})^2\pi h}{3k^2} \quad (46)$$

where D_s denotes the surface diffusivity, ζ the factor associated with the diffusion layer at the interface,[10] and $\upsilon_{||}$ the vibration frequency of structural units along the steps at the crystal surface. When $\sigma \ll 1$, we obtain

$$\sigma \approx \ln(1+\sigma) = \Delta\mu/kT \quad (47)$$

Equation 44 can be rewritten as

$$R \approx C_1\sigma^{5/6} \exp[-C_2 f(m)/T^2\sigma]\{Kf_1(m)[f(m)]^{1/2}\}^{1/3} \quad (48)$$

We notice then in case of melt growth that the crystallization driving force is normally expressed in terms of supercooling ΔT ($T_m - T$, where T_m is the melting temperature and T is the actual temperature) as

$$\Delta\mu/kT = \frac{\Delta H_m}{kT^2}\Delta T \quad (49)$$

where ΔH_m denotes the molar melting energy. From eqs 57−59, we then have

$$R = C'_1(\Delta T)^{5/6} \exp[-C'_2 f(m)/\Delta T]\{Kf_1(m)[f(m)]^{1/2}\}^{1/3} \quad (50)$$

with

$$C'_1 = C_1\left(\frac{\Delta H_m}{kT^2}\right)^{5/6} \quad \text{and} \quad C'_2 = C_2 k/\Delta H_m \quad (51)$$

2. Growth of Crystals from Vapor. In this case, the major way to transport the growth units to the kinks at the surface is via the surface diffusion. It then follows from the BCF model[10,11] that

$$V_\infty = \lambda_s\upsilon_\perp \exp(-\Delta H_{sub}/kT)\zeta'\sigma \quad (52)$$

with

$$\zeta' = (1 + D_s/\beta_{st}\lambda_s)^{-1}$$

From eqs 48, 51, and 52, the growth rate R is expressed as

$$R = C_3\sigma^{2/3}[\ln(1+\sigma)]^{1/6} \exp[-C_2 f(m,x)/T^2 \times \ln(1+\sigma)]\{Kf_1(m,x)[f(m,x)]^{1/2}\}^{1/3} \quad (53)$$

with

$$C_3 = h^{5/6}[2D_s\beta_{st}\Omega^{1/2}\upsilon_\perp/(\pi a)]^{1/3}[\lambda_s n_1\zeta' \exp(-\Delta H_{sub}/kT)]^{2/3} \quad (54)$$

(ΔH_{sub} denotes the mole energy of sublimation.) Similarly, when $\sigma \ll 1$, eq 53 is rewritten as

$$R = C_3\sigma^{5/6} \exp[-C_2 f(m)/(T^2\sigma)]\{Kf_1(m)[f(m)]^{1/2}\}^{1/3} \quad (55)$$

We notice that eqs 44, 48, 52, and 55 describe the growth kinetics of birth and spread models for both heterogeneous and homogeneous 2D nucleation. (In the case of homogeneous 2D nucleation growth, $f(m) = \{Kf_1(m)[f(m)]^{1/2}\} = 1$.) In this sense, our model covers both heterogeneous and homogeneous 2D nucleation growth.

C. Particle-Induced Surface Instability. As mentioned in the beginning, the instability of growing crystal faces is due to a certain perturbation at the growing front, which triggers rapid local growth. A foreign particle will lower the 2D nucleation barrier in the contact region, forming a so-called "2D nucleation barrier well" locally (see Figure 3) This will trigger rapid growth in the contact region, leading to surface instability.

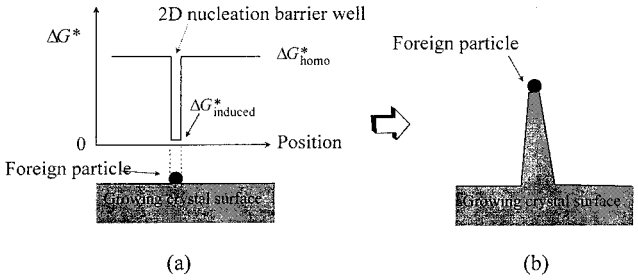

Figure 3. Illustration of the formation of "2D nucleation barrier well" and the resulting surface instability. (a) The lowering of 2D nucleation barrier in the contact region due to a foreign particle. This forms a so-called "2D nucleation barrier well" locally. (b) The rapid growth in the contact region is triggered, leading to surface instability.

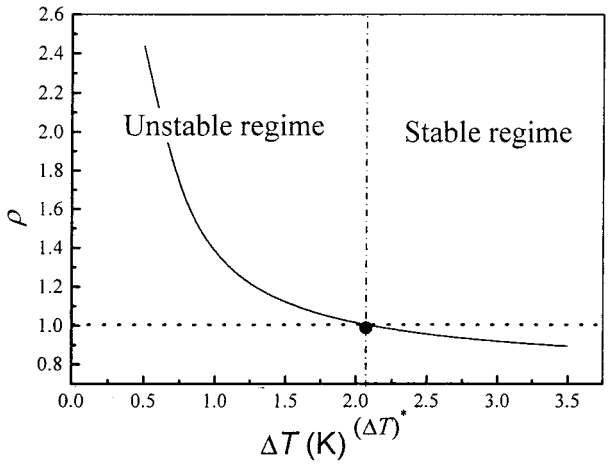

Figure 4. Plot of ρ as a function of m. At $\Delta T < (\Delta T)^*$, particle-induced surface instability occurs ($\rho > 1$). When $\Delta T \geq (\Delta T)^*$, particle-induced surface instability is then suppressed ($\rho \leq 1$).

We define the normal growth rate of the crystal surface as R_{homo} and the local rate of growth induced by foreign particles as R_{induced}. The condition for the foreign-particle-induced surface instability is $R_{\text{induced}} > R_{\text{homo}}$. To facilitate our discussion, we introduce a parameter ρ, defined as

$$\rho = \frac{R_{\text{induced}}}{R_{\text{homo}}} \tag{56}$$

Under such a definition, the particle-induced surface instability occurs when $\rho = 1$. Assuming that the normal growth is controlled by homogeneous 2D nucleation, we have for the solution growth (see eq 48)

$$\rho = Kf_1(m)[f(m)]^{1/2} \exp\{C_2[1 - f(m)]/T^2\sigma\} \tag{57}$$

and for the melt growth

$$\rho = Kf_1(m)[f(m)]^{1/2} \exp\{C'_2[1 - f(m)]/\Delta T\} \tag{58}$$

In the case of the vapor phase, an expression similar to eq 57 can be obtained.

In Figure 4, ρ is plotted versus ΔT, based on eq 58. The particle-induced surface instability will occur at $\Delta T \leq \Delta T^*$ (the unstable regime, cf. Figure 4). At $\Delta T > \Delta T^*$ (the stable regime, cf. Figure 4.), the surface instability due to foreign particles will be suppressed.

This result can be understood as follows. The occurrence of foreign particles on the growing crystal surface will on one hand lower the 2D nucleation barrier and promote the nucleation rate

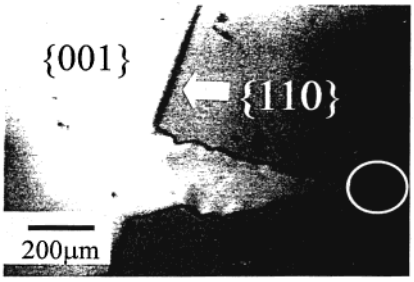

Figure 5. Surface instability induced by a solid particles at the {110} faces of naphthalene crystals.

(cf. section II.A.). On the other hand, this will reduce the effective surface area of growing embryos where growth units can be incorporated, therefore slowing the growth kinetics. At low supercoolings, the 2D nucleation barrier for a given system is relatively high. For a high nucleation rate to be achieved, lowering the nucleation barrier is the predominant factor. In this case, foreign particles (such as dust particles in our case) in contact with the surface will enhance the 2D nucleation rate and the growth rate of the crystal surface in the contact region. Conversely, at high supercoolings, the nucleation barrier is low. The transport of growth units toward the surfaces of growing embryos becomes then the predominant factor in 2D nucleation. Consequently, the normal homogeneous 2D nucleation growth becomes kinetically favored, and the particle induced surface instability will be eliminated.

We notice that for a given condition, particle-induced surface instability will occur at low supersaturations, as opposed to the surface instability caused by diffusion. Apart from this, once the particle-induced surface instability takes place, a linear relationship should be obtained between ln ρ and $1/\Delta T$ (cf. eqs 57 and 58), which does not exist when the diffusion-driven surface instability occurs.

III. Experimental Section

The crystallizing system to be examined is naphthalene. Naphthalene crystallizes in the space group $P_{2_1/a}$ with two molecules per unit cell, and the unit cell dimensions are $a = 9.253$, $b = 6.003$, $c = 9.652$, and $\beta = 123°$.[19] The crystals grown from the melt have a lozenge shape bounded by the large {001} faces on the top and the bottom and by narrow {110} faces at the sides.[20] The naphthalene used in our experiments is analytically pure (Alfa, >99.0%).

The experiments were carried out in a double-cell thermostated system,[21] where the melt and crystals were kept in the closed inner cell and the thermostated water was circulated between the inner cell and the outer cell. The cell system is placed under a Leitz transmission microscope type Divert, which is coupled with a video image processing system. For further details of experiments, see refs 20 and 21.

IV. Results and Discussion

A. Observation on Surface Instability. During the experiments, the growth of a naphthalene (110) faceted face was observed (Figure 5). At small ΔT, the local growth rate at the contact point is enhanced immediately when solid particles ($\sim$10−45 μm) come into contact with the crystal surface. It was observed that in the beginning, the faceted (110) face of naphthalene becomes convex behind the solid particle. Subsequently, the fast growth of the contact region pushes the solid particle forward into the melt, forming a fingerlike pattern (see Figure 5). The formation of fingerlike patterns is the so-called

particle-induced surface instability. The rapid growth of the finger will continue until the particle is embedded into the crystal. On the other hand, the particle-induced surface instability is completely suppressed when the supercooling ΔT is larger than a certain critical value (ΔT*).

Our experimental results indicate that the nature of the surface instability induced by solid particle is contrary to the dendritic type of surface instability described by eq 1. In our crystallization system, the heat of crystallization diffuses through the solid−fluid interface to the liquid phase. Therefore, the temperature gradient built up in the front of the growing crystal surface is always negative and becomes more negative as supercooling ΔT increases. Under the condition that the growth rate doesn't differ much, a large supercooling ΔT, corresponding to a smaller G/R at the liquid side of interface, should lead to greater surface instability (see eq 1.) However, the solid-particle-induced surface instability occurs only when G/R is greater than a certain value. This type of surface instability is completely suppressed if the supercooling is greater than this value (or G/R is more negative than the given constant).

Evidently, the solid-particle-induced surface instability and the conventional dendritic type of surface instability are two types of surface instabilities occurring in two completely different regimes.

B. Mechanism of Particle-Induced Surface Instability: Particle-Induced Growth verses Normal 2D Nucleation Growth. To verify 2D nucleation growth, we plotted $\ln[R(\Delta T)^{-5/6}]$ against $1/\Delta T$. According to eq 56, this should give rise to a linear relationship with a slope of $-C'_2$ [$f(m) = 1$] for normal homogeneous 2D nucleation growth. In the case of particle-induced heterogeneous 2D nucleation growth, the slope of the straight line is $-C'_2 f(m)$, which is less negative [$f(m) < 1$] than that of the normal homogeneous 2D nucleation growth.

For the growth of the narrow {110} faces, $\ln[R(\Delta T)^{-5/6}]$ versus $1/\Delta T$ is illustrated by curve 1 in Figure 6a, which indeed shows a linear relationship with a most negative slope. This confirms that the growth is controlled by homogenous 2D nucleation. In contact with a foreign particle, the $\ln[R(\Delta T)^{-5/6}] \sim 1/\Delta T$ plot for the tip of the finger remains linear (see curve 2 in Figure 6a). However, the slope is less negative than that of curve 1. This strongly indicates the heterogeneous 2D nucleation growth nature of the solid-induced surface instability.

Furthermore, we plot $\rho \sim 1/\Delta T$ in Figure 6b, and a straight line is obtained, as anticipated. This verifies completely our model given above.

From both the theoretical analysis and the experimental results, the particle-induced surface instability can be understood as follows: when a solid particle is in contact with a growing faceted {110} face of naphthalene crystals at low supercoolings ($\Delta T < (\Delta T)$*), the local growth rate at the contact point will be promoted. This then leads to the formation of the fingerlike growth pattern at the flat surface (see Figure 5.) When supercooling ΔT is above the critical value ($\Delta T \geq (\Delta T)$*), the heterogeneous 2D nucleation growth will become slower than the homogeneous 2D nucleation growth. The particle-induced surface instability will then be suppressed.

For the particle-induced surface instability, the critical supercooling (ΔT)* is one of the most important parameters which defines the regime where the surface instability occurs. Taking $\rho = 0$ and rearranging eq 58, we can express (ΔT)* as

$$(\Delta T)^* = C'_2[f(m) - 1]/\ln\{Kf_1(m)[f(m)]^{1/2}\} \qquad (59)$$

Obviously, according to the definitions, (ΔT)* can be calculated

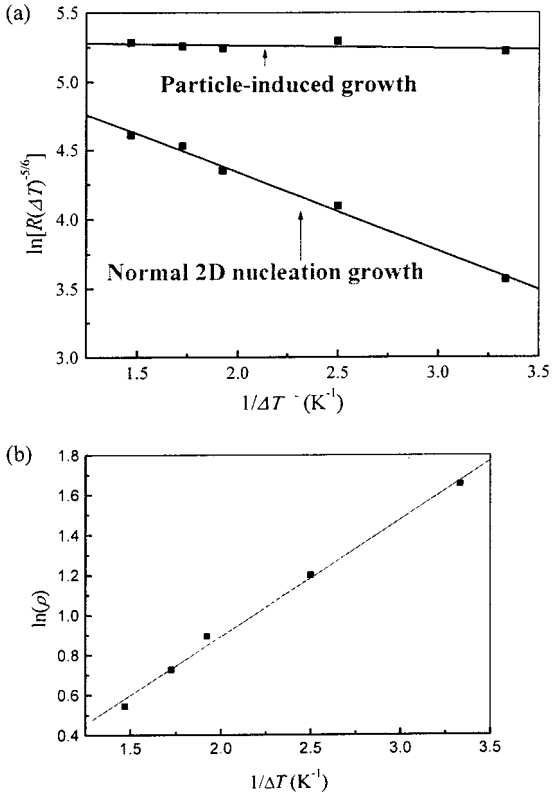

Figure 6. (a) Experimental data and the least-squares regressions of $\ln[R(\Delta T)^{-5/6}]$ vs $1/\Delta T$ of both the normal growth of {110} faces of naphthalene crystals and the particle-induced growth. (b) The plot of ln ρ vs $1/\Delta T$. The linear relationship confirms the heterogeneous 2D nucleation nature of the surface instability.

TABLE 1. Key Parameters of Particle-Induced Surface Instability for Naphthalene

parameters	(ΔT)* (K)	$f(m)^a$	m^b	$f_1(m)^c$
values	3.30	0.0352	0.847	0.179

[a] $f(m) = \text{slope}_{\text{curve1}}/\text{slope}_{\text{curve2}}$. [b] Cf. eq 9. [c] Cf. eq 39.

using the slopes and intercepts of the curved given in Figure 6a by

$$(\Delta T)^* = [\text{slope}_{\text{curve1}} - \text{slope}_{\text{curve2}}]/[\text{intercept}_{\text{curve2}} - \text{intercept}_{\text{curve1}}] \qquad (60)$$

For the naphthalene system, we obtained from eq 60 and Figure 6a $(\Delta T)^* = 3.30$ K (see Table 1). Similarly, the parameters $f(m)$, m, and $f_1(m)$ are obtained from Figure 6a. The results are also listed in Table 1.

It can be seen from this table that due to the optimal interaction ($m \rightarrow 1$), the solid particles occurring at the {110} crystal surfaces almost completely eliminate the 2D nucleation barrier of the growth, which is evidently responsible for the needlelike growth of naphthalene crystals at low supercoolings.

Apart from naphthalene, particle-induced surface instability has also been observed in many other organic crystals. Figure 7 shows such instability occurring at the {110} surface of n-$C_{32}H_{66}$. Similar to that of naphthalene, the surface instability at $\sigma < \sigma^*$ is ~1.98% (σ and σ^* are directly associated with ΔT and ΔT^* by eqs 47 and 49, respectively; see Figure 7a). When $\sigma \geq \sigma^*$, the instability is suppressed, and the faces regain the mode of faceted growth (see Figure 7b.)

We notice that the particle-induced surface instability is very often misinterpreted as the dendritic type of surface instability.

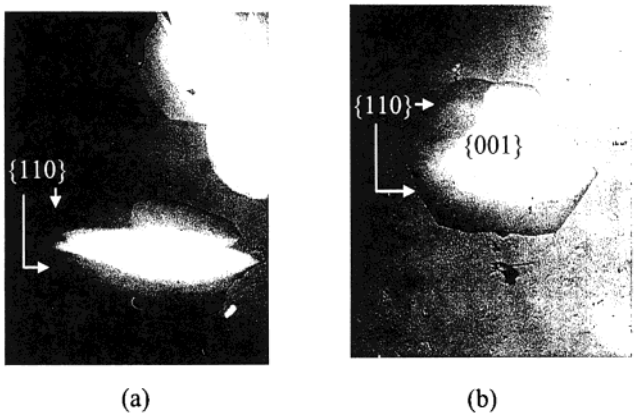

Figure 7. Surface instability induced by solid participates at the {110} faces of n-$C_{32}H_{66}$ crystals (analytically pure, Alfa, >99.0%) grown for a n-hexane solution (equilibrium temperature $T_s = 303.70$ K, spectroscopically pure, Merck, >98.0%). n-$C_{32}H_{66}$ crystals have a lozenge shape bounded by large {001} faces and narrow {110} side faces.[33] (a) The {110} faces become unstable at the supersaturation $\sigma < \sigma^*$ ($\sigma = 1.31\%$) due to the occurrence of tiny solid particles. σ and σ^* are directly associated with ΔT and ΔT^* by eqs 47 and 49, respectively). (b) At the supersaturation $\sigma > \sigma^*$ ($\sigma = 2.14\%$ and $\sigma^* = 1.98\%$), the instability is suppressed, and the {110} faces remain as flat faces during the growth.

These confusions mislead in most cases our understanding and prevent us from the effective control for such surface instability. From this perspective, the results given in this paper are extremely important to clarify such confusions.

References and Notes

(1) Huang, S. C.; Glicksman, M. E. *Acta Metall*. **1981**, *29*, 717−734.
(2) Langer, J. S. *Rev. Mod. Phys.* **1980**, *52*, 1−28.
(3) Kepler, J. *De Nive Sexangula*; Hardie, C., Transl.; Clarendon: Oxford, 1966; p 1611.
(4) Chernov, A. A. *J. Cryst. Growth* **1974**, *24/25*, 11.
(5) Kessler, D. A.; Koplik, J.; Levine, H. *Adv. Phys.* **1988**, *37*, 255−339.
(6) Langer, J. S. *Science* **1989**, *243*, 1150−1156.
(7) Ben-Jacob, E.; Garik, P. *Nature* **1990**, *343*, 523−350.
(8) Brener, E. A.; Melnikov, V. I. *Adv. Phys.* **1991**, *40*, 53−91.
(9) Ben-Jocob, E. *Contemp. Phys.* **1993**, *34*, 247−273.
(10) Chernov, A. A. *Modern Crystallography III-Crystal Growth*; Springer-Verlag: Berlin, 1984.
(11) Bennema, P.; Gilmer, G. H. In *Crystal Growth: An Introduction*; Hartman, P., Ed.; North-Holland: Amsterdam, 1973; p 263.
(12) Bennema, P. In *Handbook on Crystal Growth*; Hurle, D. T. J., Ed.; North-Holland: Amsterdam, 1993; p 477.
(13) Burton, W. K.; Cabrera, N. *Discuss. Faraday Soc.* **1949**, *5*, 33−40. Burton, W. K.; Cabrera, N.; Frank, F. C. *Phil. Trans. R. Soc. London, Ser. A* **1951**, *243*, 299−358.
(14) Mutaftschiev, B. In *Handbook of Crystal Growth*; Hurle, D. T. J., Ed.; North-Holland: Amsterdam, 1993; pp 187−248. Mullin, J. W. *Crystallization*; Butterworth-Heinemann: Woburn, MA, 1997.
(15) Liu, X. Y.; Maiwa, K.; Tsukamoto, K. *J. Chem. Phys.* **1997**, *106*, 1870.
(16) Nielsen, R. In *International Series of Monographs on Analytical Chemistry*; Belcher, R., Gordon, L., Eds.; Pergamon Press: New York, 1964; Vol. 1.
(17) Mutaftschiev, B. In *Handbook on Crystal Growth*; Hurle, D. T. J., Ed.; North-Holland: Amsterdam, 1993; p 187. Fowler, S. R.; Guggenhein, E. A. *Statistical Thermodynamics*; Cambridge University: London, 1960.
(18) McDonald, J. E. *Am. J. Phys.* **1962**, *30*, 870.
(19) Cruickshank, D. W. J. *Acta Crystallogr.* **1957**, *10*, 504.
(20) Jetten, L. A. M. J.; Human, H. J.; Bennema, P.; van der Eerden, J. P. *J. Cryst. Growth* **1984**, *68*, 5030.
(21) Liu, X. Y. *Phys Rev. B* **1993**, *48*, 1825.
(22) Liu, X. Y.; Bennema, P.; van der Eerden, J. P. *Nature* **1992**, *356*, 778.
(23) Chernov, A. A. *Modern Crystallography III-Crystal Growth*; Springer-Verlag: Berlin, 1984.
(24) Bennema, P. In *Handbook of Crystal Growth*; Hurle, D. T. J., Ed.; North-Holland: Amsterdam, 1993; 476−581.
(25) Kosterlitz, J. M.; Thouless, D. J. *J. Phys. C* **1973**, *6*, 1181−1203.
(26) Kosterlitz, J. M. *J. Phys. C* **1974**, *7*, 1046−1060.
(27) Liu, X. Y.; van Hoof, P.; Bennema, P. *Phys. Rev. Lett.* **1993**, *71*, 109.
(28) Knops, H. J. F. *Phys. Rev. Lett.* **1977**, *39*, 766. Jose, J. V.; Kadanoff, L. P.; Kirkpatrick, S.; Nelson, D. R. *Phys. Rev. B* **1977**, *16*, 1217.
(29) Nozieres, P.; Gallet, F. *J. Phys.* (*Paris*) **1987**, *48*, 353−367.
(30) Elwenspoek, M.; van der Eerden, J. P. *J. Phys. A* **1987**, *20*, 669−678.
(31) Elwenspoek, M.; Boerhof, W. *Phys. Rev. B* **1987**, *36*, 5326−5329.
(32) Liu, X. Y.; Bennema, P. *J. Cryst. Growth* **1993**, *129*, 69−74.
(33) Bennema, P.; Liu, X. Y.; Lewtas, K.; Tack, R. D.; Rijpkema, J. J. M.; Roberts, K. J. *J. Cryst. Growth* **1992**, *121*, 679.